Journal of Thermal Analysis and Calorimetry (2019) 137:1809–1825
https://doi.org/10.1007/s10973-019-08078-y

Effect of magnetic field on laminar forced convective heat transfer of MWCNT–Fe_3O_4/water hybrid nanofluid in a heated tube

Jalal Alsarraf[1] · Reza Rahmani[2] · Amin Shahsavar[2] · Masoud Afrand[3] · Somchai Wongwises[4,5] · Minh Duc Tran[6,7]

Received: 9 December 2018 / Accepted: 8 February 2019 / Published online: 20 February 2019

Abstract

A numerical investigation is carried out to assess the hydrothermal performance of a water-based hybrid nanofluid containing both Fe_3O_4 (magnetite) nanoparticles and carbon nanotubes (CNTs) in a heated tube in the presence of a constant non-uniform magnetic field. The magnetic field is created by three pairs of permanent magnets. The effects of Reynolds number, magnetite, and CNT volume concentrations as well as magnetic field strength are investigated. The acquired data for the case of without magnetic field confirmed higher values of heat transfer and pressure drop as a result of utilizing nanofluid compared with water. Additionally, it was found that the Nusselt number and pressure drop of the studied nanofluid samples increase significantly under the magnetic field. Moreover, the influence of magnetic field increases with an increase in the nanoparticle concentrations and magnetic field strength and decrease in the Reynolds number. The maximum increments of 109.31% and 25.02% in comparison with the case of without field were obtained in the average Nusselt number and pressure drop for hybrid nanofluid containing 0.9% magnetite and 1.35% CNT at Reynolds number of 500.

Keywords Ferrofluid · Carbon nanotube · Hybrid nanofluid · Convective heat transfer · Magnetic field

Introduction

A heat exchanger is a device designed to efficiently transfer thermal energy from one fluid to another. They are utilized in many industrial processes from geothermal and fossil power generation to refrigeration and desalination. Because of these applications, the development of new-generation heat exchangers and their innovative applications and the subsequent improvement in the efficiency of heat exchangers have always been one of the concerns of researchers. So far, various methods have been proposed to augment the performance of heat exchangers including extended surfaces, inserts, coiled or twisted tubes, surface treatments, suction, and injection.

Water, deionized water, glycol/water solutions, and silicon oil are the heat transfer fluids most commonly used in heat exchangers. The main drawback of these fluids is their low thermal conductivity which reduces the hydrothermal performance of heat exchangers. This problem has led to the notion of adding solid metallic and metal oxide nanoadditives of very high thermal conductivity to

✉ Minh Duc Tran
tranminhduc@tdtu.edu.vn

1 Automotive and Marine Engineering Department, College of Technological Studies (CTS), Public Authority for Applied Education and Training (PAAET), Shuwaikh 70654, Kuwait

2 Department of Mechanical Engineering, Kermanshah University of Technology, Kermanshah, Iran

3 Department of Mechanical Engineering, Najafabad Branch, Islamic Azad University, Najafabad, Iran

4 Fluid Mechanics, Thermal Engineering and Multiphase Flow Research Lab. (FUTURE), Department of Mechanical Engineering, Faculty of Engineering, King Mongkut's University of Technology Thonburi, Bangmod, Bangkok 10140, Thailand

5 The Academy of Science, The Royal Society of Thailand, Sanam Suea Pa, Dusit, Bangkok 10300, Thailand

6 Division of Computational Mechatronics, Institute for Computational Science, Ton Duc Thang University, Ho Chi Minh City, Vietnam

7 Faculty of Electrical and Electronics Engineering, Ton Duc Thang University, Ho Chi Minh City, Vietnam

common heat transfer fluids. In 1995, Choi [1] was able to prepare these fluids for the first time, which he called "nanofluids." Several researchers have evaluated the performance of heat exchangers filled with nanofluids from the first-law and second-law points of view. Shahsavar et al. [2] conducted simulations to examine the impact of nanoadditive volume fraction on the friction and heat transfer irreversibilities during flow of aqueous magnetite–CNT hybrid nanofluid inside a tube-in-tube heat exchanger. The findings revealed that the total irreversibility boosts with augmenting the volume fraction of CNT and Fe_3O_4 nanoadditives. Bhanvase et al. [3] experimentally investigated the hydrothermal performance of a vertical helically coiled tube heat exchanger filled with the water-based PANI (polyaniline) nanofluid. They reported that increasing the volume fraction of nanoadditive and Reynolds number causes an increase in the mean heat transfer coefficient. In experimental work, Hosseinian et al. [4] studied the impact of surface vibration on enhancing the stability and heat transfer coefficient of water–CNT nanofluid in a flexible double-pipe heat exchanger. They found that the heat transfer coefficient augments by applying vibration on the outer surface of heat exchanger.

Ferrofluids or magnetic nanofluids include surfactant-coated nanoparticles in a liquid medium which can be controlled magnetically. A stable ferrofluid is produced by capping the magnetic nanoparticles with a layer of surfactant or polymers that provide electrostatic or steric repulsion between the particles, thus preventing their agglomeration and resultant settling [5].

Plenty of efforts have been focused on the investigation of nanofluids in recent years by many researchers [6–15]. However, only very few works have been reported on the convective heat transfer of ferrofluids through a pipe [16–20]. Yarahmadi et al. [16] studied the effects of a water–magnetite ferrofluid on the laminar forced convective heat transfer in a heated tube for constant and oscillating magnetic fields experimentally. Different parameters including nanoparticle concentration, Reynolds number, magnetic field strength, and arrangement as well as the kind of magnetic field were examined. They showed an improvement in the heat transfer characteristics of the ferrofluid which is more pronounced using an alternating magnetic field compared with a constant magnetic field. Besides, higher effect of magnetic field was achieved for higher nanoparticles volume concentration and lower Reynolds number. Asfer et al. [17] conducted experiments on laminar forced convective heat transfer characteristics of the water–magnetite ferrofluid flowing in a heated tube in the presence of permanent magnets. They reported that several issues affect the improvement in ferrofluid convective heat transfer, i.e., (a) the strength of magnetic force compared with the inertia force, (b) interaction of ferrofluid flow with the aggregation of nanoparticles at the tube wall near the magnets, and (c) the chain-like structures of nanoparticles within the ferrofluid. Hatami et al. [18] surveyed the impacts of a uniform magnetic field on the laminar forced convective heat transfer of water–magnetite ferrofluid passing through a heated tube. The results revealed a reduction in the convective heat transfer coefficient in the presence of a magnetic field by increasing the nanoparticles concentration, while it is boosted for the case of without magnetic field. Mokhtari et al. [19, 20] conducted a 3-D numerical analysis of water–magnetite ferrofluid in a heated tube equipped with a non-uniform twisted tape. They assessed heat transfer by the influence of nanoparticle concentration, magnetic field intensity, twisted tape shape, and Reynolds number. They found that the application of magnetic field and twisted tape significantly increases the average Nusselt number of water–magnetite ferrofluid.

In recent years, the study of new generation of nanofluids including various combinations of different kind of nanoparticles, called hybrid nanofluids, is more attended to enhance the heat transfer [2, 21–23]. The suspensions of magnetite–CNT hybrid nanoparticles have been widely studied as hybrid nanofluids due to the advantageous effects of magnetite and CNT, recently. Baby and Sundara [24] studied the thermal conductivity of magnetite–CNT/water hybrid nanofluid. They presented enhancements of 3–5% and 6.5–10% on the thermal conductivity at 0.005% and 0.03% volume concentrations of magnetite and CNT in the hybrid nanofluid, respectively, in the temperature range of 30–50 °C compared with the base fluid. Felicia and Philip [5] investigated the magnetorheological properties of magnetite–CNT/oil hybrid nanofluid. The results revealed an enhancement in the viscosity due to the formation of heterogeneous structures such as chains and columns in the presence of magnetic field. Sundar et al. [25] evaluated experimentally the hydrothermal characteristics of magnetite–CNT/water hybrid nanofluid passing through a tube. They demonstrated that for the Reynolds number of 3000, 14.81% improvement occurred in the Nusselt number for 0.3% concentration of nanoparticle. Shahsavar et al. [26] analyzed laminar convective heat transfer of magnetite–CNT/water hybrid nanofluid in a heated tube in the presence of constant and alternating magnetic fields. They showed higher increment of heat transfer for a constant magnetic field compared with an alternating magnetic field. Harandi et al. [27] determined the thermal conductivity of magnetite–CNT/ethylene glycol hybrid nanofluid in terms of temperature (25–50 °C) and concentration (0–2.3%). They found higher thermal conductivity of nanofluid for higher temperature and concentration of nanoparticles.

The aim of this investigation is to analyze the effect of an external magnetic field produced by permanent magnets on the laminar forced convective heat transfer and pressure drop characteristics of a water-based magnetite/CNT hybrid nanofluid flowing through a horizontal heated tube. The results are compared with the pure water and also with the case of without magnetic field. For this purpose, the magnetite and CNT concentrations and strength of the magnetic field and the Reynolds number are investigated. To the best knowledge of the authors, the detailed behavior of the laminar forced convective heat transfer and pressure drop of magnetite–CNT/water hybrid nanofluids in the presence of an external magnetic field emitted by permanent magnets is first studied in this paper.

Characteristics of the hybrid nanofluid

The hybrid nanofluid examined in this study is a suspension of gum arabic (GA)-coated CNTs and tetramethylammonium hydroxide (TMAH)-coated magnetite nanoparticles in pure water. The nanofluid is prepared by mixing and sonication of the required amount of magnetite–water ferrofluid and CNT–water nanofluid. The magnetite–water ferrofluid and the CNT–water nanofluid are prepared according to the method suggested by Berger et al. [28] and Garg et al. [29], respectively. The details of the preparation method and characterization of this hybrid nanofluid are not described here and can be found in the author's previous work [30]. The TMAH and GA molecules are interacted causing the attachment of the magnetite and CNT nanoparticles observed in Fig. 1.

After careful preparation and characterization, a series of experiments are performed to obtain the thermophysical properties of the nanofluids containing different concentrations of the magnetite and CNT nanoparticles. The volume concentration of the magnetite and CNT nanoparticles in the prepared nanofluid samples as well as the density (ρ), specific heat (c_p), viscosity (), and thermal conductivity (k) of these hybrid nanofluids are presented in Table 1. A liquid density gravity meter (DA-130N, KEN, Japan) and a differential scanning calorimeter (DSC, Q20, TA Instruments, USA) are used to measure the nanofluid density and specific heat, respectively. The viscosity and thermal conductivity of the hybrid nanofluid samples are measured using a Paar Physica MCR 300 parallel disk rheometer and a KD2-pro instrument (Decagon devices, Inc., USA).

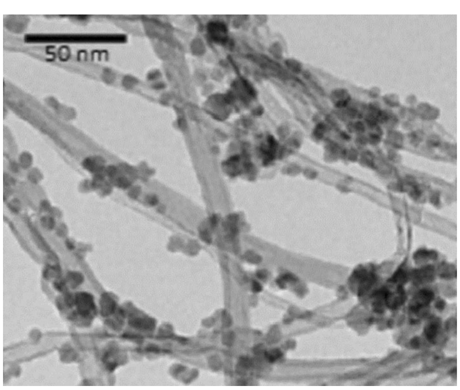

Fig. 1 TEM image of water-based hybrid nanofluid [2]

Model description

Geometry and boundary conditions

The horizontal straight tube with 1.25 m length and 4.8 mm diameter is heated by a uniform heat flux of 1000 W m^{-2}. The flow is considered steady state and laminar. Uniform velocity and uniform temperature (25 °C) at the inlet and zero relative pressure at the outlet are considered. No-slip condition is also employed on the tube wall.

Three pairs of NdFeB permanent magnets with opposite poles facing each other are placed on both sides of the tube to generate three-dimensional magnetic field. These magnets have a length of 12 cm, width of 6 cm, and thickness of 2.5 cm. The distance between the centers of three pairs of permanent magnets form the tube inlet is 16, 56, and 96 cm, respectively. The schematic of the problem along with the arrangement of the permanent magnets is given in Fig. 2.

Mathematical modeling

The conservation of mass, momentum, and energy should be solved to investigate the laminar forced convective heat transfer of magnetic nanofluids under the influence of a magnetic field. The assumptions to write the mentioned equations are:

- Considering constant thermophysical properties for the water-based hybrid nanofluid.
- Negligible effects of the buoyancy compared with the forced convection and hydromagnetic effects.
- Considering the hybrid nanofluid as a homogeneous single-phase fluid.

Therefore, the governing equations can be expressed as follows:

$$\nabla.\vec{V} = 0 \tag{1}$$

Table 1 Properties of the studied nanofluid samples

Sample name	Fe_3O_4/vol%	CNT/vol%	ρ/kg m^{-3}	C_p/J kg^{-1} K^{-1}	η/kg m^{-1} s^{-1}	k/W m^{-1} K^{-1}
0.5%FF	0.5	0	1016.77	4093.83	0.001042	0.695
0.5%FF + 0.25%CNT	0.5	0.25	1019.52	4076.20	0.001193	0.754
0.5%FF + 0.5%CNT	0.5	0.5	1022.28	4058.66	0.001236	0.765
0.5%FF + 0.75%CNT	0.5	0.75	1025.04	4041.22	0.001262	0.769
0.7%FF	0.7	0	1024.67	4060.29	0.001300	0.728
0.7%FF + 0.35%CNT	0.7	0.35	1028.53	4035.95	0.001480	0.787
0.7%FF + 0.7%CNT	0.7	0.7	1032.39	4011.79	0.001527	0.809
0.7%FF + 1.05%CNT	0.7	1.05	1036.25	3987.81	0.001570	0.831
0.9%FF	0.9	0	1032.58	4027.27	0.001534	0.749
0.9%FF + 0.45%CNT	0.9	0.45	1037.54	3996.40	0.001755	0.839
0.9%FF + 0.9%CNT	0.9	0.9	1042.50	3965.83	0.001804	0.856
0.9%FF + 1.35%CNT	0.9	1.35	1047.47	3935.55	0.001855	0.887

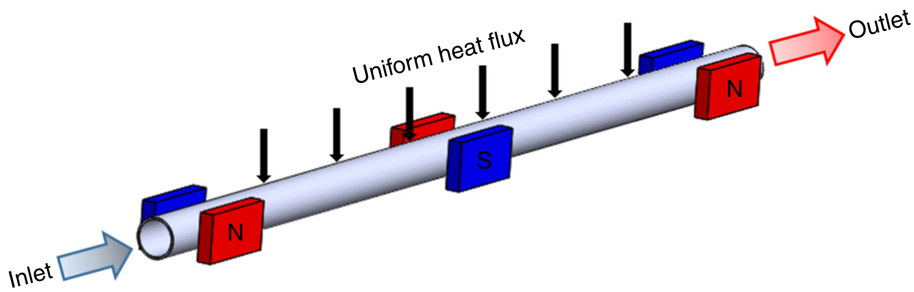

Fig. 2 Schematic of the studied problem

$$\rho\frac{D\vec{V}}{Dt} = -\nabla p + \eta\nabla^2\vec{V} + (\vec{M}.\nabla)\vec{B} \quad (2)$$

$$\rho c_p\frac{DT}{Dt} = k\nabla^2 T - \mu_0 T\frac{\partial\vec{M}}{\partial T}\left[(\vec{V}.\nabla)\vec{H}\right] \quad (3)$$

where $\vec{V}$ is the velocity, T is the temperature, p is the pressure, $\vec{M}$ is the magnetization, and $\vec{B}$ is the magnetic field intensity.

The last term on the right-hand side of Eq. (2) is called Kelvin body force regarding the effect of spatially non-uniform magnetic field.

The relation between $\vec{M}$ and magnetic field vector ($\vec{H}$) is as follows [31]:

$$\vec{M} = \chi_m\vec{H} \quad (4)$$

where

$$\chi_m = \frac{\chi_0}{1+\beta(T-T_0)} \quad (5)$$

is the total magnetic susceptibility, χ_0 is the differential magnetic susceptibility, β is the thermal expansion coefficient of the ferrofluid, and T_0 is the reference temperature.

The vectors of magnetic field intensity, magnetization, and magnetic field are related as [31]:

$$\vec{B} = \mu_0(\vec{M}+\vec{H}) = \mu_0(1+\chi_m)\vec{H} \quad (6)$$

where μ_0 is magnetic permeability in vacuum.

Therefore, the Kelvin body force is given as [32]:

$$\vec{F} = \mu_0\chi_m(1+\chi_m)\left(\vec{H}.\vec{\nabla}\right)\vec{H} = \frac{1}{2}\mu_0\chi_m(1+\chi_m)\vec{\nabla}(\vec{H}.\vec{H}) + \mu_0\chi_m\vec{H}\left(\vec{H}.\vec{\nabla}\chi_m\right). \quad (7)$$

Magnetic field simulation

Distribution of the magnetic field for the given configuration of the permanent magnets is simulated using COMSOL Multiphysics. Figure 3 shows the z-component of the magnetic flux density along the tube centerline. The maximum intensity of the magnetic field occurs near the magnets and decays with distance from them. Consequently, the magnetic flux density has six peaks of 1000 Gauss along the tube centerline.

Data reduction

The Reynolds number for the pipe flow is defined as:

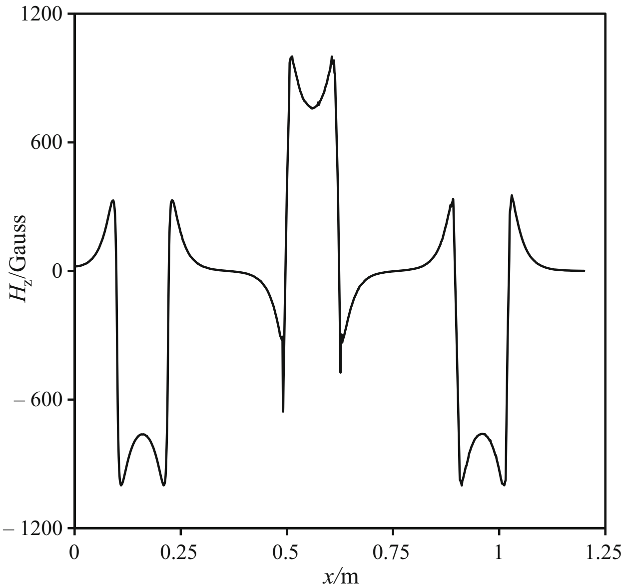

Fig. 3 Variation of the magnetic flux density norm along the tube centerline

$$Re = \frac{\rho v_{\mathrm{in}} D}{\eta} \quad (8)$$

where v_{in} is the inlet velocity and D is the tube diameter.

The local convective heat transfer coefficient is given as:

$$h(x) = \frac{q''}{T_{\mathrm{w}}(x) - T_{\mathrm{nf}}(x)} \quad (9)$$

where q'' is the wall heat flux, x is the axial distance from the tube inlet, T_{w} is the wall temperature, and T_{nf} is the bulk temperature of the nanofluid.

The convective heat transfer coefficient is also defined in the form of Nusselt number as:

$$Nu(x) = \frac{h(x)D}{k_{\mathrm{w}}} \quad (10)$$

where k_{w} is the thermal conductivity of the pure water at 25 °C.

The average Nusselt number is computed by integrating the local values along the tube wall as:

$$\overline{Nu} = \frac{1}{L}\int_0^L Nu(x)\mathrm{d}x. \quad (11)$$

The performance index is a flow criterion which examines the Nusselt number enhancement of nanofluid compared to the base fluid at equal pumping power, which is computed as [33]:

$$\mathrm{PI} = \frac{(Nu/Nu_{\mathrm{bf}})}{(f/f_{\mathrm{bs}})^{1/3}} \quad (12)$$

where f is the friction factor defined as $f = \frac{64}{Re}$ [33].

Numerical method and validation

A FORTRAN computer code is developed to solve the governing Eqs. (1)–(3) along with the aforementioned boundary conditions using finite volume method (FVM). The grid layout is arranged by utilizing collocated grid procedure, while Quick scheme is adopted for the convection–diffusion terms. The velocity and pressure coupling is solved using the SIMPLEC algorithm, and the Rhie–Chow interpolation is used to eliminate any non-physical pressure oscillations. Additionally, the results of the magnetic field distribution obtained using COMSOL Multiphysics are passed to the FORTRAN code with a text file.

In this study, as shown in Fig. 4, a structured non-uniform mesh was generated with higher density near the wall where the velocity and temperature gradients vary rapidly in the domain. For independency analysis between the grid and the numerical results and choosing an appropriate mesh configuration, several combinations of node numbers have been examined by comparing the dimensionless axial velocity profile at the cross section of $x = 1.2$ m and average Nusselt number for the flow of 0.9%FF + 1.35% CNT at $Re = 150$ for the magnetic field strength of 1000 Gauss. The comparison of velocity profiles is depicted in Fig. 5 showing a little variation between different studied mesh results. Besides, Table 2 shows that the variation between the average Nusselt number between cases 5 and 6 is 0.17%. Therefore, the mesh consisting of $250 \times 60 \times 40$ (250, 60 and 40 nodes in axial, radial, and circumferential directions, respectively) is used for the rest of simulations.

The accuracy of the numerical solution is validated by comparing the results for the Nusselt number with well-

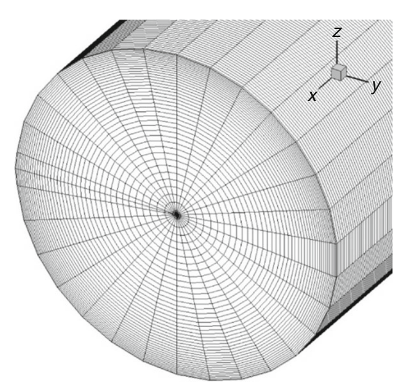

Fig. 4 Structured non-uniform grid for the computational domain

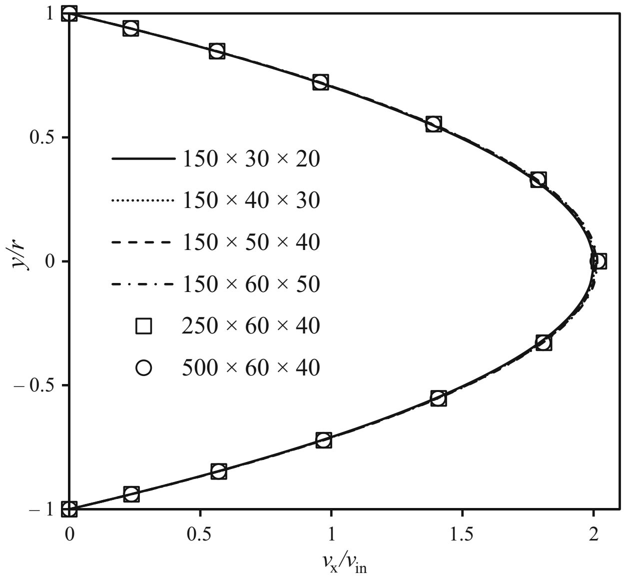

Fig. 5 Grid size independency for the dimensionless axial velocity profile at cross section x = 1.2 m for flow of 0.9%FF + 1.35%CNT at Re = 150 in the presence of a magnetic field with the maximum strength of 1000 Gauss

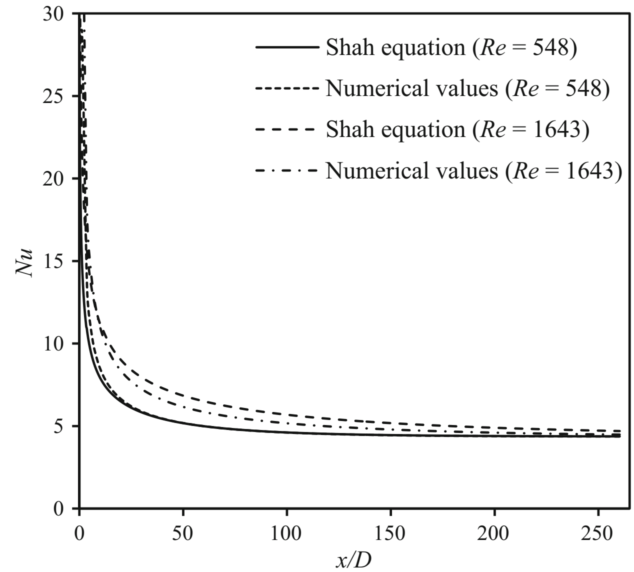

Fig. 6 Comparison between the obtained Nusselt number of the pure water in the present work and results of Shah equation [33, 34]

Table 2 Effect of grid size on the average Nusselt number for flow of 0.9%FF + 1.35%CNT at Re = 150 in the presence of a magnetic field with the maximum strength of 1000 Gauss

Grid size	150 × 30 × 20	150 × 40 × 30	150 × 50 × 40	150 × 60 × 50	250 × 60 × 40	500 × 60 × 40
$\overline{Nu}$	10.32	10.81	11.1	11.4	11.6	11.62

known equation of Shah [34, 35] for laminar tube flows with a constant heat flux as:

$$Nu(x) = \begin{cases} 1.302x_*^{-1/3} - 1, & x_* \leq 0.00005 \\ 1.302x_*^{-1/3} - 0.5, & 0.00005 \leq x_* \leq 0.0015 \\ 4.364 + 8.68(10^3 x_*)^{-0.506} e^{-41x_*}, & x_* \geq 0.0015 \end{cases} \quad (13)$$

where $x_* = [(x/D)/(Re.Pr)]$. The results, as shown in Fig. 6, indicate that the obtained Nusselt numbers are in reasonable agreement compared with Shah equation.

The numerical solution is further validated against experimental data by Azizian et al. [36] in terms of local Nusselt number of water–magnetite ferrofluid in the presence of magnetic field of three pairs of permanent magnets. This comparison is demonstrated in Fig. 7, and it can be observed that there is a suitable consistency between the results.

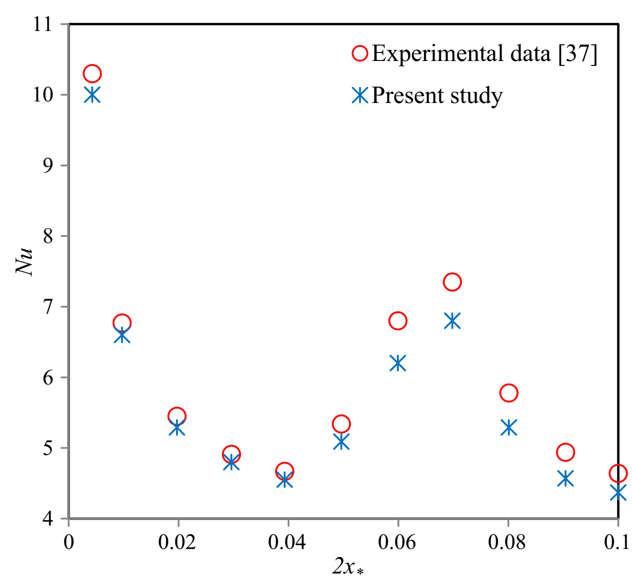

Fig. 7 Comparison between the obtained Nusselt number of the water–magnetite ferrofluid in the present work and experimental results of Azizian et al. [36]

Results and discussion

Hydrothermal characteristics of Fe_3O_4/CNT hybrid nanofluid without a magnetic field

The variations of the local Nusselt number in terms of the dimensionless axial distance from tube inlet for the pure ferrofluids, hybrid nanofluids, and water as base fluid at $Re = 500$ in the absence of a magnetic field are shown in Fig. 8. The Nusselt number exhibits the same behavior for all the considered cases. It has a high value at the tube inlet, which diminishes as the distance from the inlet increases. The reason for this phenomenon is that the thickness of the thermal boundary layer at tube inlet is small, and the gradual increase in this thickness leads to the reduction in temperature gradient and, consequently, the reduction in convective heat transfer coefficient and Nusselt number. The results also indicate that the local Nusselt number of all the examined ferrofluids is higher than that of the water. Furthermore, increasing the concentrations of magnetite and CNT leads to an increase in the local Nusselt number. Regarding Eq. (10), the local Nusselt number is a function of the thermal conductivity coefficient of water, tube diameter, and convective heat transfer coefficient. The water thermal conductivity and tube diameter are constant, and therefore, the difference between the local Nusselt numbers of various nanofluids and water is only due to the difference between the convective heat transfer coefficients which are related to the thermal conductivity directly. The results presented in Table 1 show that an increase in magnetite and CNT concentrations leads to an increase in thermal conductivity coefficient and, consequently, convective heat transfer coefficient. Therefore, the higher local Nusselt numbers of the examined nanofluids compared with the water can be attributed to their greater thermal conductivity coefficient.

Table 3 presents the enhancement percentage in the average Nusselt number of the examined nanofluids relative to that of the water at different Reynolds numbers. The average Nusselt number of 0.5%FF, 0.7%FF, and 0.9%FF at the Reynolds numbers of 500–2000 is 17.25–18.7%, 20.17–27.25%, and 23.18–38.83% greater than that of the water, respectively. Besides, an average Nusselt number enhancement of 17.45–19.57% and 23.51–52.54% is observed at 0.5%FF + 0.25%CNT and 0.9%FF + 1.35% CNT, respectively, in the Reynolds number range of 500–2000 compared to the water. A review of the published literature reveals that the average Nusselt number of magnetite–water ferrofluid flowing in a heated tube has only been investigated in two works: the authors previous work [26]; and Ghofrani et al. [37]. Ghofrani et al. [37] reported an increase of 12% in the average Nusselt number of the nanofluid with 1% concentration compared with the water without a magnetic field. The discrepancy between the results of Ghofrani et al. [37] and the findings of the

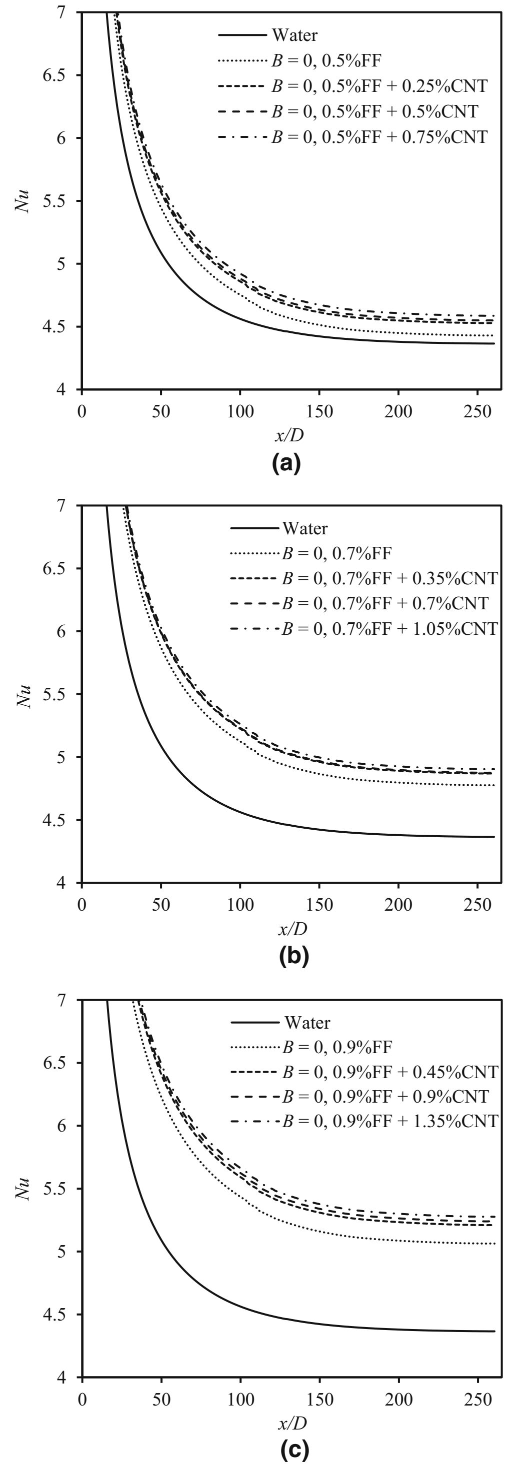

Fig. 8 Local Nusselt number of pure ferrofluid and hybrid nanofluids containing **a** 0.5%FF, **b** 0.7%FF and **c** 0.9% FF and different amounts of CNTs in terms of the dimensionless axial distance from the tube entrance at $Re = 500$ in the absence of a magnetic field

Table 3 Enhancement percentage in the average Nusselt numbers of the examined nanofluids relative to that of the water at different Reynolds numbers

Sample	*Re* = 500	*Re* = 1000	*Re* = 1500	*Re* = 2000
0.5%FF	17.25	17.66	18.18	18.70
0.5%FF + 0.25%CNT	17.45	17.98	18.71	19.57
0.5%FF + 0.5%CNT	17.72	18.72	20.05	21.65
0.5%FF + 0.75%CNT	18.34	19.67	21.47	23.74
0.7%FF	20.17	21.95	24.27	27.25
0.7%FF + 0.35%CNT	21.02	23.40	26.48	30.36
0.7%FF + 0.7%CNT	21.26	24.29	28.28	33.36
0.7%FF + 1.05%CNT	21.46	25.22	30.32	36.98
0.9%FF	23.18	26.90	31.90	38.83
0.9%FF + 0.45%CNT	23.20	28.28	34.91	43.56
0.9%FF + 0.9%CNT	23.24	28.70	36.34	46.66
0.9%FF + 1.35%CNT	23.51	29.84	39.41	52.54

present research is probably due to the factors such as the diameter of nanoparticles and the quality of the synthesized ferrofluids. The explanation for the improvement in heat transfer with an increase in the Reynolds number is that an increase in Reynolds number leads to increasing the flow velocity causing a reduction in the velocity boundary layer and thus the thermal boundary layer. Therefore, the temperature gradient and the degree of heat transfer increases.

In addition to the enhancement of heat transfer, the use of nanofluids increases the pressure drop, which is deemed undesirable due to an increase in the required pumping power. Table 4 schematizes the pressure drop of the examined nanofluids at various Reynolds numbers. The results of the well-known Darcy's equation [38] for the pressure drop in circular pipe fully developed laminar flows ($\Delta p = f \frac{L}{D} \frac{\rho V^2}{2}$, where V is the mean flow velocity) are also included in Table 4. There is a good agreement between the results obtained from the developed code in this study and those obtained from Darcy's equation. The use of a nanofluid leads to a considerable increase in pressure loss, which becomes worse with increasing concentrations of magnetite and CNT. The results indicate that the pressure drop of 0.5%FF, 0.7%FF, and 0.9%FF at Reynolds numbers of 500–2000 is 31.28–38.1%, 106.82–110.88%, and 185.16–190.48% greater than those of the water, respectively. Additionally, a pressure drop increment of 73.96–78.78% and 314.49–321.77% is observed at 0.5%FF + 0.25%CNT and 0.9%FF + 1.35% CNT, respectively, at the Reynolds number of 500–2000 compared with the water. At a constant Reynolds number, higher concentration of nanoparticles leads to a higher flow velocity and a lower thickness of velocity boundary layer which results in a higher velocity gradient and thus a higher of pressure drop. Moreover, the findings reveal that increasing the Reynolds number leads to a higher pressure drop due to an increase in flow velocity.

Table 4 Pressure drop of the examined nanofluids at different Reynolds numbers

Sample	Present work				Darcy's equation			
	Re = 500	*Re* = 1000	*Re* = 1500	*Re* = 2000	*Re* = 500	*Re* = 1000	*Re* = 1500	*Re* = 2000
Water	147	292	436	579	144	288	432	576
0.5%FF	203	397.2	582.2	760.12	193.1	386.2	579.3	772.5
0.5%FF + 0.25%CNT	262.8	513.9	751.1	1007.2	252.5	504.9	757.4	1009.8
0.5%FF + 0.5%CNT	280	550.2	805.2	1061	270.3	540.5	810.8	1081
0.5%FF + 0.75%CNT	289	560.1	845	1126.7	281	556.2	843	1123.9
0.7%FF	310	609.7	899.9	1197.5	298.3	596.5	894.8	1193.1
0.7%FF + 0.35%CNT	396.6	785.8	1166.1	1549.6	385.1	770.3	1155.4	1540.5
0.7%FF + 0.7%CNT	428	839.2	1245.3	1637.2	408.5	816.9	1225.4	1633.8
0.7%FF + 1.05%CNT	449	876.7	1299.4	1734.3	430.2	860.3	1290.5	1720.7
0.9%FF	427	838.9	1242.3	1651.1	412.1	824.3	1236.4	1648.5
0.9%FF + 0.45%CNT	557	1092.9	1619.9	2156.6	536.9	1073.7	1610.6	2147.4
0.9%FF + 0.9%CNT	587.7	1149.3	1704.5	2266.5	564.6	1129.1	1693.7	2258.2
0.9%FF + 1.35%CNT	620	1211.1	1792.2	2399.9	594.1	1188.2	1782.3	2376.4

Table 5 Performance index of the examined nanofluids at different Reynolds numbers in the absence of magnetic field

Sample	*Re* = 500	*Re* = 1000	*Re* = 1500	*Re* = 2000
0.5%FF	1.161	1.171	1.183	1.195
0.5%FF + 0.25%CNT	1.167	1.178	1.194	1.199
0.5%FF + 0.5%CNT	1.171	1.186	1.207	1.226
0.5%FF + 0.75%CNT	1.180	1.204	1.217	1.238
0.7%FF	1.195	1.216	1.244	1.273
0.7%FF + 0.35%CNT	1.202	1.231	1.265	1.303
0.7%FF + 0.7%CNT	1.206	1.237	1.280	1.335
0.7%FF + 1.05%CNT	1.207	1.250	1.304	1.369
0.9%FF	1.222	1.267	1.321	1.390
0.9%FF + 0.45%CNT	1.225	1.281	1.351	1.436
0.9%FF + 0.9%CNT	1.226	1.285	1.365	1.467
0.9%FF + 1.35%CNT	1.227	1.296	1.396	1.523

According to the above discussion, it can be concluded that the use of nanofluid leads to the simultaneous increase in the heat transfer and pressure drop, which the former is desired, and the latter is undesirable. Therefore, in order to evaluate the merit of using the nanofluid instead of pure water, the parameter PI is employed. As mentioned earlier, this parameter shows the changes in the convective heat transfer coefficient and friction factor of the nanofluid compared with the pure water. In fact, PI values higher than 1 indicates that an increase in the nanoparticles to the base fluid enhances heat transfer more than pressure drop. Table 5 illustrates the PI of the examined nanofluids at various Reynolds numbers. It is evident that for all states, the PI of nanofluid is larger than 1 and increases with an increase in the concentrations of magnetite and CNT and Reynolds number. Therefore, in the absence of magnetic field, the use of nanofluid has a greater merit at higher Reynolds numbers and nanoparticle concentrations.

Hydrothermal characteristics of Fe_3O_4/CNT hybrid nanofluid under a magnetic field

In this section, the influences of the magnetic field induced by three pairs of permanent magnets on the heat transfer, pressure drop, and performance index of pure ferrofluids and hybrid nanofluids containing various magnetite and CNT concentrations are investigated. Three pairs of permanent magnets with the maximum strength of 1000 Gauss are placed along the tube which causes a normal magnetic field to the flow direction of magnetic nanofluids. The fluctuations of Kelvin force along the tube centerline and along the radial directions of y and z, for tube cross section at x = 0.56 m (center of the second pair of magnets), are given in Fig. 9a–c, respectively. The fluctuations of magnetic flux density are severe near the edges of magnets, and the severity of fluctuations diminishes at the mid-regions of magnets. Therefore, the gradient of magnetic flux density is large near the edges and small at the mid-regions of magnets. So, considering the direct relationship that exists between the Kelvin force and the gradient of magnetic flux density, a large force is expected to be applied to ferrofluid near the edges of magnets, which should diminish in intensity at the mid-regions of magnets. This prediction is confirmed by Fig. 9a. When the ferrofluid moving along the tube axis approaches a magnet, a large force is exerted on it along the axial direction which causes the ferrofluid to be trapped at each magnet position. As illustrated in Fig. 9b, c, simultaneous forces are also applied on ferrofluid along the y and z directions; which push the ferrofluid toward the tube wall.

Figures 10 and 11, respectively, illustrate the contours of axial velocity and temperatures at six different cross sections ($x = 0.16$ m, $x = 0.36$ m, $x = 0.56$ m, $x = 0.76$ m, $x = 0.96$ m, and $x = 1.16$ m) for 0.9%FF + 1.35%CNT and Reynolds number of 500 in the cases of with and without magnetic field. It is clear that in the absence of magnetic field, the counters of axial velocity and temperature have regular patterns so that the velocity is the lowest adjacent to the tube wall and increases toward the center of the tube, while the opposite is true about the temperature. In addition, after a certain distance from the tube inlet, the velocity contour does not change which is due to the fact that the flow is developed. As is observed in Figs. 10 and 11, the application of magnetic field results in the significant changes in the flow and the temperature fields. The large Kelvin body force causes the nanofluid to move toward the tube wall and thereby cooling it.

The variation of the local Nusselt number in terms of the non-dimensional axial distance from tube inlet for the pure ferrofluids and hybrid nanofluids in the presence of magnetic field is illustrated in Fig. 12 at the Reynolds number of 500. To highlight the effect of magnetic field on the local Nusselt number of the examined nanofluids, the results related to the case of without magnetic field are also

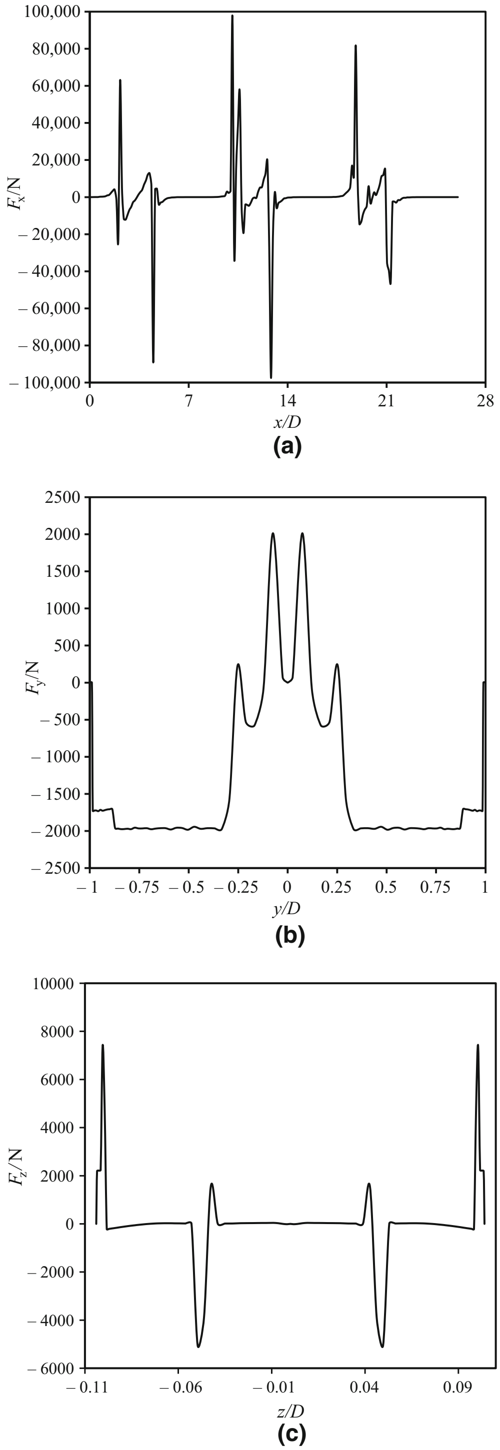

Fig. 9 Kelvin force distribution **a** along the center line of the pipe in x direction, **b** in radial direction along the y direction at $x = 0.56$ m and **c** in radial direction along the z direction at $x = 0.56$ m for 0.9%FF + 1.35%CNT at $Re = 500$

presented in these figures. The local Nusselt number increases at the edges of each magnet, and the rate of increase diminishes by moving away from the edges due to the presence of a large Kelvin force near the edges. The results reveal that, with the application of a magnetic field, the local Nusselt number of all nanofluid increases follows a steeper slope as the magnetite and CNT concentrations increase. This observation is consistent with the findings of Asfer et al. [17] and Azizian et al. [36].

Former research works have presented contradictory results regarding the effect of a constant magnetic field on the forced convective heat transfer of ferrofluids flowing in heated tubes. Some researchers have reported the reduction in convective heat transfer using a constant magnetic field [16, 37], while others have claimed the enhancement of convective heat transfer coefficient [26, 36, 39]. The most popular mechanism proposed in the literature to explain the improvement in ferrofluids' heat transfer in the presence of a constant magnetic field is the aggregation of magnetic nanoparticles in the direction of magnetic field; which, on the one hand, leads to a higher thermal conductivity coefficient due to the formation of low thermal resistance pathways, and, on the other hand, results in the generation of turbulent thermal boundary layer and thus increasing the convective heat transfer. The results provided by Hong et al. [40] indicate that the increase in the ferrofluids' thermal conductivity coefficient in the presence of a magnetic field is a very time-consuming process, and that, considering the short time that ferrofluid is exposed to the magnetic field in the tube (less than 10 s), it seems that increasing the convective heat transfer of ferrofluids exposed to a magnetic field cannot be attributed to the increase in the thermal conductivity coefficients. Yarahmadi et al. [16] suggested that the improvement/reduction in the convective heat transfer of ferrofluids exposed to a constant magnetic field depends on the relative effects of three factors: a higher thermal conductivity coefficient, a lower thermal boundary layer thickness, and a higher of viscosity. The first two of these factors lead to an increase in heat transfer, while the third factor reduces the degree of heat transfer. They stated that in magnetic fields of low intensity, the increase in viscosity plays a more dominant role and causes a reduction in the ferrofluid convective heat transfer, while in magnetic fields of higher intensity, the effects of the increase in thermal conductivity and reduction in thermal boundary layer thickness overcome the effect of a higher viscosity and cause enhancement of convective heat transfer.

In Table 6, the enhancement percentage in the average Nusselt number of the examined nanofluids in the presence of magnetic field compared with the case of without magnetic field is presented. The heat transfer enhancement improves with enhancement of magnetite and CNT concentrations and diminishes with an increase in Reynolds number. Increasing the Reynolds number speeds up the flow and thus reduces their exposure time to the magnetic

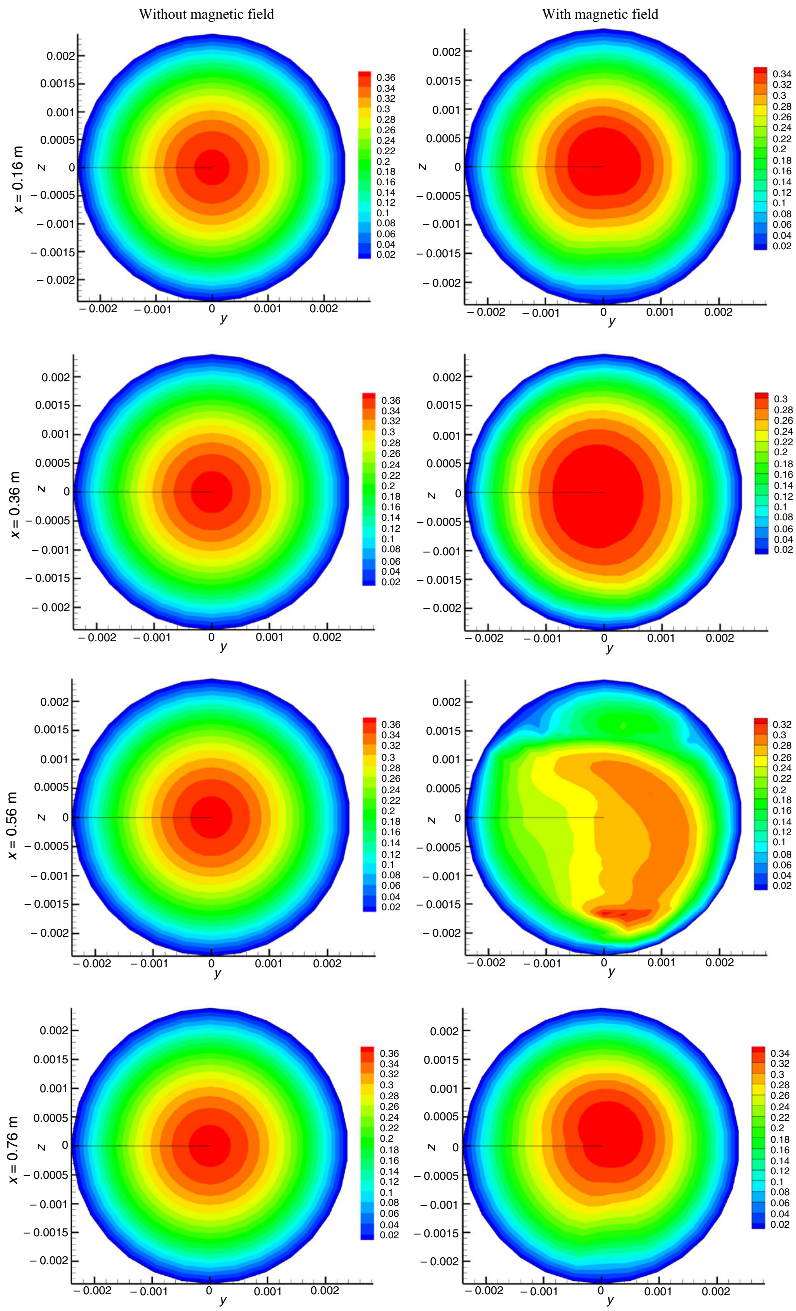

Fig. 10 Contour of axial velocity at different cross sections for 0.9%FF + 1.35%CNT and Reynolds number of 500 in the cases of with and without magnetic field

field. For example, the application of a magnetic field with the maximum strength of 1000 Gauss in the Reynolds number range of 500–2000 causes 78.48–0.34% enhancement in the average Nusselt number of 0.9%FF, while the amount of enhancement for 0.9%FF + 1.35%CNT is 109.31–1.11%.

The increase in the convective heat transfer capacity of ferrofluids due to the application of a magnetic field is valuable only when it does not lead to a significant increase in pressure loss. The percent increase in the pressure loss of the examined nanofluids exposed to a magnetic field with the maximum strength of 1000 Gauss at the Reynolds number of 500, compared with the case of no magnetic field, is reported in Table 7. The application of the magnetic field leads to a higher pressure loss, which augments with increasing the magnetite and CNT concentrations.

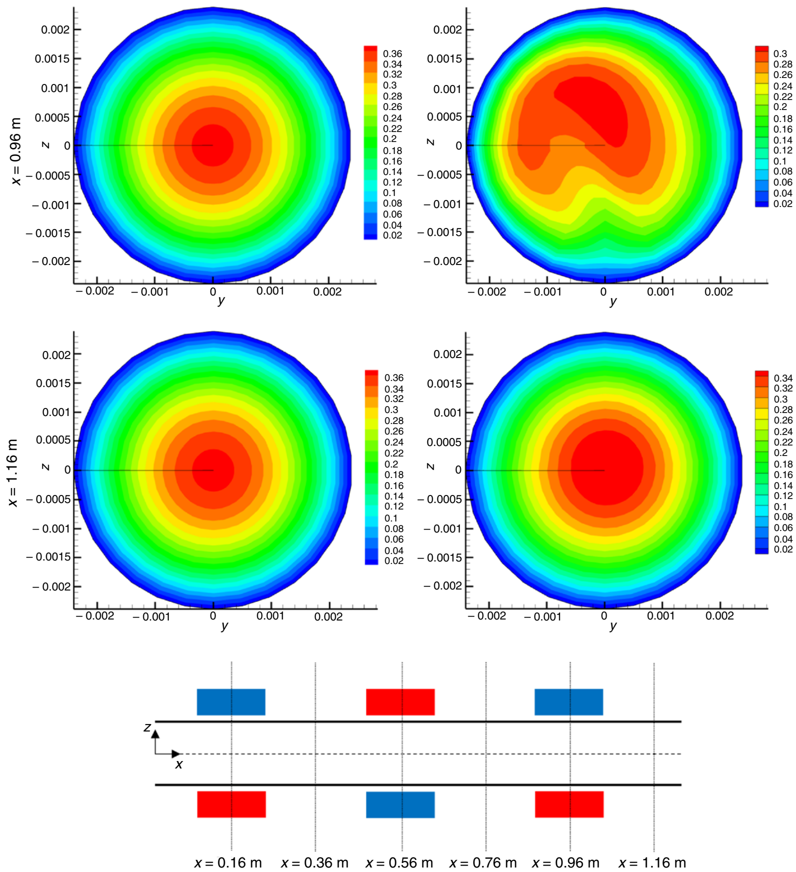

Fig. 10 continued

According to the results, the application of a magnetic field increases the pressure loss of 0.5%FF and 0.9%FF by 15.47% and 18.48%, compared with the case of no magnetic field, while the increase in the pressure loss of 0.5%FF + 0.25%CNT and 0.9%FF + 1.35%CNT amounts to 18.66% and 25.02%, respectively. The increase in pressure drop under the effect of magnetic field can be attributed to the presence of Kelvin force along different directions, which blocks the passage of ferrofluid and deflects it toward the tube wall.

Table 8 depicts the PI of the considered nanofluids in the presence of magnetic field with the maximum strength of 1000 Gauss at the Reynolds number of 500. It is seen that for all states, the PI of nanofluid is greater than 1 and intensifies by boosting the concentrations of magnetite and CNT nanoparticles. The maximum PI is equal to 2.382 which belongs to 0.9%FF + 1.35%CNT. In addition, it is observed that the PI of the studied nanofluids in the presence of magnetic field is higher as compared with the case of no magnetic field. Consequently, it can be said that the application of magnetic nanofluid has a greater merit in the presence of magnetic field.

Finally, Fig. 13 displays the influence of the strength of the magnetic field on the local Nusselt number of 0.9%FF + 1.35%CNT at the Reynolds number of 500. The decrease in magnetic field strength reduces the effect of magnetic field on the local Nusselt number. According to the results, the average Nusselt number of 0.9%FF + 1.35%CNT under the effect of magnetic field with the maximum strength of 1000, 700, and 500 Gauss is 109.31%, 58.01%, and 27.61% greater than that for the case of without magnetic field, respectively. The reduction in magnetic field intensity reduces the turbulence of the thermal boundary layer, as a result of which the improvement of heat transfer declines.

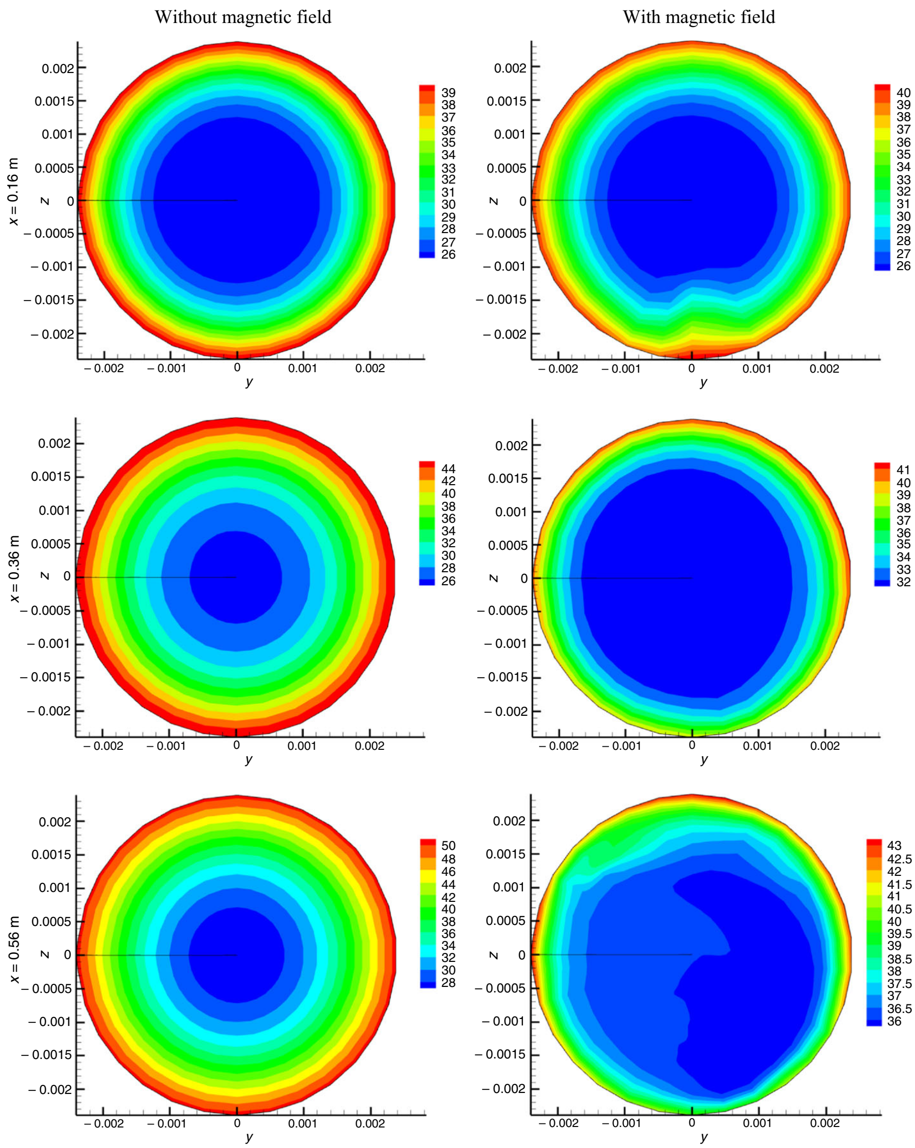

Fig. 11 Contour of temperature at different cross sections for 0.9%FF + 1.35%CNT and Reynolds number of 500 in the cases of with and without magnetic field

Conclusions

The laminar forced convective heat transfer and pressure drop of the MWCNT–Fe_3O_4/water hybrid nanofluid flowing inside a heated tube under the effect of an external non-uniform magnetic field induced by three pairs of permanent magnets was investigated. The effects of the magnetite and CNT nanoparticle concentrations, Reynolds number, and magnetic field strength were also studied. The following results are obtained:

- Without a magnetic field, increasing the Fe_3O_4 and CNT concentrations and Reynolds number leads to an increase in the average Nusselt number and pressure drop of the studied nanofluid samples. The highest enhancement in the average Nusselt number and pressure drop compared with that of the water is 52.54% and 2376.4%, respectively, which belong to 0.9%FF + 1.35%CNT at $Re = 500$.
- The heat transfer performance augments by the application of a magnetic field and the amount of enhancement increases for higher magnetic field strength and

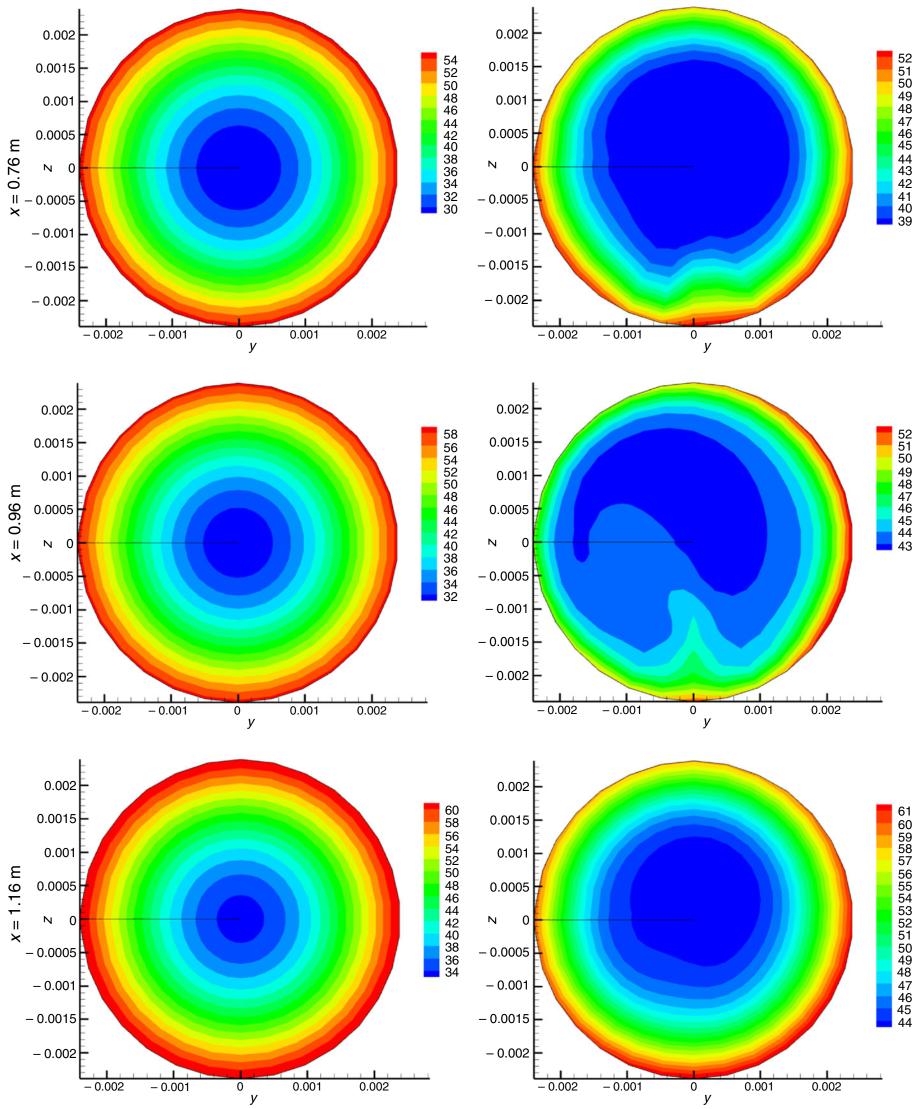

Fig. 11 continued

nanoparticle concentration and reduces for higher Reynolds numbers. The highest enhancement relative to the without magnetic field case is 109.31% which belongs to 0.9%FF + 1.35%CNT at $Re = 500$ and magnetic field strength of 1000 Gauss.

- Application of a constant non-uniform magnetic field leads to an increase in the pressure loss of the studied nanofluid samples and the amount of enhancement augments with an increase in nanoparticle concentration. The maximum increment is 25.02% for 0.9%FF + 1.35%CNT at $Re = 500$.

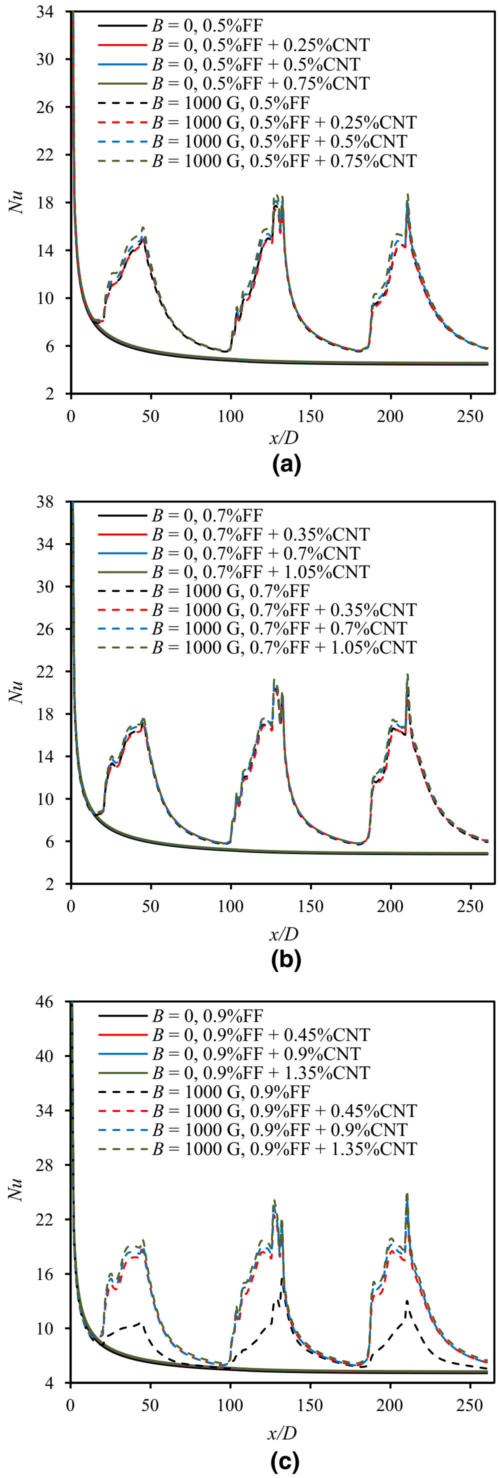

Fig. 12 Local Nusselt number of pure ferrofluid and hybrid nanofluids containing **a** 0.5%FF, **b** 0.7%FF and **c** 0.9% FF and different amounts of CNTs in terms of the dimensionless axial distance from the tube entrance at $Re = 500$ in the presence of a magnetic field

Table 6 Magnetic-field-induced enhancement (%) in the average Nusselt number of the studied nanofluid samples with respect to the case of without magnetic field at various Reynolds numbers

Sample	Re = 500	Re = 1000	Re = 1500	Re = 2000
0.5%FF	78.48	11.21	0.76	0.34
0.5%FF + 0.25%CNT	79.43	11.87	0.83	0.39
0.5%FF + 0.5%CNT	82.05	11.99	0.89	0.42
0.5%FF + 0.75%CNT	85.35	12.11	0.94	0.44
0.7%FF	92.88	13.12	1.10	0.56
0.7%FF + 0.35%CNT	93.92	13.45	1.21	0.59
0.7%FF + 0.7%CNT	95.00	13.88	1.34	0.63
0.7%FF + 1.05%CNT	97.43	14.11	1.44	0.69
0.9%FF	104.63	15.65	1.99	0.91
0.9%FF + 0.45%CNT	105.32	15.99	2.12	0.99
0.9%FF + 0.9%CNT	107.05	16.23	2.34	1.01
0.9%FF + 1.35%CNT	109.31	16.73	2.65	1.11

Table 7 Enhancement percentage in the pressure drop of the examined nanofluids under the effect of a magnetic field with the maximum strength of 1000 Gauss at the Reynolds number of 500 compared to the case of without magnetic field

Sample	$\frac{\left[(\Delta p)_{\text{with magnetic field}} - (\Delta p)_{\text{without magnetic field}}\right] \times 100}{(\Delta p)_{\text{without magnetic field}}}$
0.5%FF	15.47
0.5%FF + 0.25%CNT	18.66
0.5%FF + 0.5%CNT	19.61
0.5%FF + 0.75%CNT	20.72
0.7%FF	16.75
0.7%FF + 0.35%CNT	18.88
0.7%FF + 0.7%CNT	19.74
0.7%FF + 1.05%CNT	23.66
0.9%FF	18.48
0.9%FF + 0.45%CNT	22.86
0.9%FF + 0.9%CNT	23.8
0.9%FF + 1.35%CNT	25.02

Table 8 Performance index of the examined nanofluids at different Reynolds numbers in the presence of magnetic field

Sample	PI
0.5%FF	1.975
0.5%FF + 0.25%CNT	1.978
0.5%FF + 0.5%CNT	2.009
0.5%FF + 0.75%CNT	2.055
0.7%FF	2.188
0.7%FF + 0.35%CNT	2.209
0.7%FF + 0.7%CNT	2.207
0.7%FF + 1.05%CNT	2.218
0.9%FF	2.349
0.9%FF + 0.45%CNT	2.361
0.9%FF + 0.9%CNT	2.370
0.9%FF + 1.35%CNT	2.382

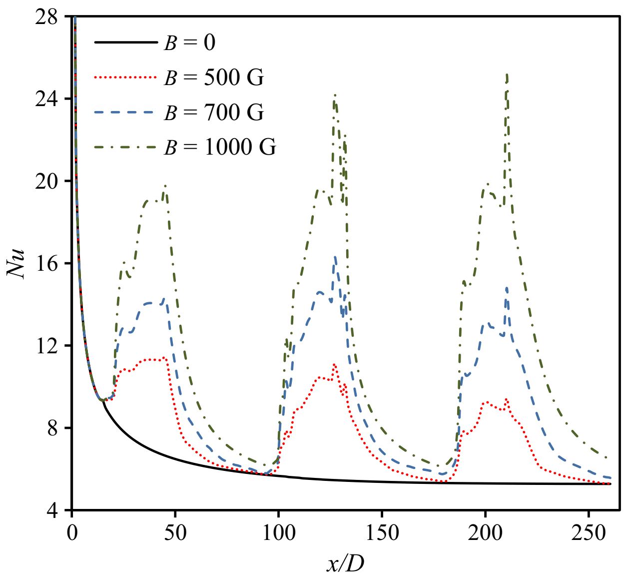

Fig. 13 Local Nusselt number of 0.9%FF + 1.35%CNT against the dimensionless axial distance from the tube entrance at *Re* = 500 in the presence of a magnetic field with three magnetic strengths of 500, 700 and 1000 Gauss

Acknowledgements The fifth author acknowledges the support provided by the ''Research Chair Grant'' National Science and Technology Development Agency (NSTDA) and King Mongkut's University of Technology Thonburi through the ''KMUTT 55th Anniversary Commemorative Fund''.

References

1. Choi SUS. Enhancing thermal conductivity of fluids with nanoparticles. ASME J Heat Transf. 1995;66(1995):99–105.
2. Shahsavar A, Rahimi Z, Bahiraei M. Optimization of irreversibility and thermal characteristics of a mini heat exchanger operated with a new hybrid nanofluid containing carbon nanotubes decorated with magnetic nanoparticles. Energy Convers Manag. 2017;150:37–47.
3. Bhanvase BA, Sayankar SD, Kapre A, Fule PJ, Sonawane SH. Experimental investigation on intensified convective heat transfer coefficient of water based PANI nanofluid in vertical helical coiled heat exchanger. Appl Therm Eng. 2018;128:134–40.
4. Hosseinian A, Meghdadi Isfahani AH, Shirani E. Experimental investigation of surface vibration effects on increasing the stability and heat transfer coefficient of MWCNTs–water nanofluid in a flexible double pipe heat exchanger. Exp Therm Fluid Sci. 2018;90:275–85.
5. Felicia LJ, Philip J. Magnetorheological properties of a magnetic nanofluid with dispersed carbon nanotubes. Phys Rev E. 2014;89:022310.
6. Popplewell J, Al-Qenaie A, Charles SW, Moskowitz R, Raj K. Thermal conductivity measurements on ferrofluids. Colloid Polym Sci. 1982;260:333–8.
7. Shahsavar A, Salimpour MR, Saghafian M, Shafii MB. An experimental study on the effect of ultrasonication on thermal conductivity of ferrofluid loaded with carbon nanotubes. Thermochim Acta. 2015;617:102–10.
8. Malvandi A, Heysiattalab S, Ganji DD. Effects of magnetic field strength and direction on anisotropic thermal conductivity of ferrofluids (magnetic nanofluids) at filmwise condensation over a vertical cylinder. Adv Powder Technol. 2016;27:1539–46.
9. Amani M, Amani P, Kasaeian A, Mahian O, Wongwises S. Thermal conductivity measurement of spinel-type ferrite $MnFe_2O_4$ nanofluids in the presence of a uniform magnetic field. J Mol Liq. 2017;230:121–8.
10. Shahsavar A, Khanmohammadi S, Karimipour A, Goodarzi M. A novel comprehensive experimental study concerned synthesizes and prepare liquid paraffin-Fe_3O_4 mixture to develop models for both thermal conductivity & viscosity: a new approach of GMDH type of neural network. Int J Heat Mass Transf. 2019;131:432–41.
11. Esfe MH, Hajmohammad MH, Razi P, Ahangar MRA, Arani AAA. The optimization of viscosity and thermal conductivity in hybrid nanofluids prepared with magnetic nanocomposite of nanodiamond cobalt-oxide (ND-Co3O4) using NSGA-II and RSM. Int Commun Heat Mass Transf. 2016;79:128–34.
12. Amani M, Amani P, Kasaeian A, Mahian O, Wongwises S. Experimental study on viscosity of spinel-type manganese ferrite nanofluid in attendance of magnetic field. J Magn Magn Mater. 2017;428:457–63.
13. Shahsavar A, Khanmohammadi S, Toghraie D, Salehipour H. Experimental investigation and develop ANNs by introducing the suitable architectures and training algorithms supported by sensitivity analysis: measure thermal conductivity and viscosity for liquid paraffin based nanofluid containing Al_2O_3 nanoparticles. J Mol Liq. 2019;276:850–60.
14. Mahian O, Kolsi L, Amani M, Estelle P, Ahmadi G, Kleinstreuer C, Marshall JS, Siavashi M, Taylor RA, Niazmand H, Wongwises S, Hayat T, Kolanjiyil A, Kasaeian A, Pop I. Recent advances in modeling and simulation of nanofluid flows-part I: fundamentals and theory. Phys Rep. 2018. https://doi.org/10.1016/j.physrep.2018.11.004.
15. Mahian O, Kolsi L, Amani M, Estelle P, Ahmadi G, Kleinstreuer C, Marshall JS, Taylor RA, Abu-Nada E, Rashidi S, Niazmand H, Wongwises S, Hayat T, Kasaeian A, Pop I. Recent advances in modeling and simulation of nanofluid flows-part II: applications. Phys Rep. 2018;15:12. https://doi.org/10.1016/j.physrep.2018.11.003.
16. Yarahmadi M, Moazami Goudarzi H, Shafii MB. Experimental investigation into laminar forced convective heat transfer of ferrofluids under constant and oscillating magnetic field with different magnetic field arrangements and oscillation modes. Exp Therm Fluid Sci. 2015;68:601–11.

17. Asfer M, Mehta B, Kumar A, Khandekar S, Panigrahi PK. Effect of magnetic field on laminar convective heat transfer characteristics of ferrofluid flowing through a circular stainless steel tube. Int J Heat Fluid Flow. 2016;59:74–86.
18. Hatami N, Kazemnejad Banari A, Malekzadeh A, Pouranfard AR. The effect of magnetic field on nanofluids heat transfer through a uniformly heated horizontal tube. Phys Lett A. 2017;381:510–5.
19. Shahsavar A, Ansarian R, Bahiraei M. Effect of line dipole magnetic field on entropy generation of Mn–Zn ferrite ferrofluid flowing through a minichannel using two-phase mixture model. Powder Technol. 2018;340:370–9.
20. Mokhtari M, Hariri S, Gerdroodbary B, Yeganeh R. Effect of non-uniform magnetic field on heat transfer of swirling ferrofluid flow inside tube with twisted tapes. Chem Eng Process. 2017;117:70–9.
21. Shahsavar A, Bahiraei M. Experimental investigation and modeling of thermal conductivity and viscosity for non-Newtonian hybrid nanofluid containing coated CNT/Fe_3O_4 nanoparticles. Powder Technol. 2017;318:441–50.
22. Bahiraei M, Berahmand M, Shahsavar A. Irreversibility analysis for flow of a non-Newtonian hybrid nanofluid containing coated CNT/Fe_3O_4 nanoparticles in a minichannel heat exchanger. Appl Therm Eng. 2017;125:1083–93.
23. Hemmat Esfe M, Alirezaie A, Rejvani M. An applicable study on the thermal conductivity of SWCNT–MgO hybrid nanofluid and price-performance analysis for energy management. Appl Therm Eng. 2017;111:1202–10.
24. Baby TT, Sundara R. Surfactant free magnetic nanofluids based on core–shell type nanoparticle decorated multiwalled carbon nanotubes. J Appl Phys. 2011;110:064325.
25. Sundar LS, Singh MK, Sousa ACM. Enhanced heat transfer and friction factor of MWCNT–Fe_3O_4/water hybrid nanofluids. Int Commun Heat Mass Transf. 2014;52:73–83.
26. Shahsavar A, Saghafian M, Salimpour MR, Shafii MB. Experimental investigation on laminar forced convective heat transfer of ferrofluid loaded with carbon nanotubes under constant and alternating magnetic fields. Exp Therm Fluid Sci. 2016;76:1–11.
27. Harandi SS, Karimipour A, Afrand M, Akbari M, D'Orazio A. An experimental study on thermal conductivity of F-MWCNTs–Fe_3O_4/EG hybrid nanofluid: effects of temperature and concentration. Int Commun Heat Mass Transf. 2016;76:171–7.
28. Berger P, Adelman NB, Beckman KJ, Campbell DJ, Ellis AB, Lisensky GC. Preparation and properties of an aqueous ferrofluid. J Chem Educ. 1999;76:943–8.
29. Garg P, Alvarado JL, Marsh C, Carlson TA, Kessler DA, Annamalai K. An experimental study on the effect of ultrasonication on viscosity and heat transfer performance of multi-wall carbon nanotube-based aqueous nanofluids. Int J Heat Mass Transf. 2009;52:5090–101.
30. Shahsavar A, Saghafian M, Salimpour MR, Shafii MB. Effect of temperature and concentration on thermal conductivity and viscosity of ferrofluid loaded with carbon nanotubes. Heat Mass Transf. 2015. https://doi.org/10.1007/s00231-015-1743-8.
31. Strek T, Jopek H. Computer simulation of heat transfer through a ferrofluid. Phys Status Solidi (b). 2007;244:1027–37.
32. Ganguly R, Sen S, Puri IK. Heat transfer augmentation using a magnetic fluid under the influence of a line dipole. J Magn Magn Mater. 2004;271:63–73.
33. Shahsavar A, Rahimi Z, Salehipour H. Nanoparticle shape effects on thermal-hydraulic performance of boehmite alumina nanofluid in a horizontal double-pipe minichannel heat exchanger. Heat Mass Transf. 2019. https://doi.org/10.1007/s00231-018-02558-x.
34. Shah RK, London AL. Laminar flow forced convection in ducts, supplement 1 to advances in heat transfer. New York: Academic Press; 1978.
35. Shah RK, Bhatti MS. Laminar convective heat transfer in ducts. In: Kakac S, Shah RK, Aung W, editors. Handbook of single-phase convective heat transfer. New York: Wiley; 1987 **(Chapter 3)**.
36. Azizian R, Doroodchi E, McKrell T, Buongiorno J, Hu LW, Moghtaderi B. Effect of magnetic field on laminar convective heat transfer of magnetite nanofluids. Int J Heat Mass Transf. 2014;68:94–109.
37. Ghofrani A, Dibaei MH, Hakim Sima A, Shafii MB. Experimental investigation on laminar forced convection heat transfer of ferrofluids under an alternating magnetic field. Exp Therm Fluid Sci. 2013;49:193–200.
38. Lienhard JH IV, Lienhard JH V. Heat transfer textbook. 2nd ed. Cambridge: Phlogiston Press; 2002.
39. Goharkhah M, Salarian A, Ashjaee M, Shahabadi M. Convective heat transfer characteristics of magnetite nanofluid under the influence of constant and alternating magnetic field. Powder Technol. 2015;274:258–67.
40. Hong H, Wright B, Wensel J, Jin S, Ye XR, Roy W. Enhanced thermal conductivity by the magnetic field in heat transfer nanofluids containing carbon nanotube. Synth Metals. 2007;157:437–40.